FURTHER IN SITU DATA SUPPORT LOW ABUNDANCE OF ^{60}FE IN THE EARLY SOLAR SYSTEM. J. Kodolányi[1], P. Hoppe[1], C. Vollmer[2], and J. Berndt[2], [1]Max Planck Institute for Chemistry (Hahn-Meitner-Weg 1, 55128 Mainz, Germany; j.kodolanyi@mpic.de), [2]University of Münster, Institute for Mineralogy (Corrensstrasse 24, 48149 Münster, Germany).

Introduction: The early Solar System abundance of the short-lived radioactive isotope ^{60}Fe (t½ = 2.62 million years; [1]) is important for planetary evolution models, because it bears on the role of ^{60}Fe as a heat source for differentiation [2]. To estimate ^{60}Fe abundance at Solar System birth, [3–10] studied early Solar System rocks using in situ and bulk analytical techniques. These investigations yielded systematically different results. Whereas most estimates of the ^{60}Fe/^{56}Fe ratio at the time canonical calcium-aluminum-rich inclusions (CCAIs) formed (^{60}Fe/^{56}Fe$_{CCAI}$) are below 2×10^{-8} based on bulk isotope data (MC-ICP-MS; [4–6]), the in situ measurements (SIMS, NanoSIMS) of several chondrules and chondritic troilite suggested ^{60}Fe/^{56}Fe$_{CCAI}$ ratios of 10^{-7}–10^{-6} [3,7–10]. Nevertheless, the bulk analyses of minimally altered quenched angrites and basaltic eucrites yielded precise isochrons with comparable ^{60}Fe/^{56}Fe$_{CCAI}$ ratios (~10^{-8}; [4–6]), and the most recent bulk and in situ measurements of chondrules failed to confirm the highest ^{60}Fe/^{56}Fe$_{CCAI}$ ratios of earlier in situ studies [6,10,11]. Thus, a low abundance of ^{60}Fe in the early Solar System, i.e., one in accordance with the levels estimated based on bulk isotope data, is more likely.

Two notable exceptions of the bulk rock datasets are those of [12] and [13]. These authors estimated ^{60}Fe/^{56}Fe$_{CCAI}$ ratios of 7.5 (±3.3) $\times 10^{-8}$, and 6.4 (±1.0) $\times 10^{-7}$ (uncertainties throughout the abstract are 1σ, i.e., at the 68 % confidence level), based on ^{60}Ni-deficits in IVB and IID iron meteorites, which have subchondritic Fe/Ni ratios. Especially the latter ratio is remarkable, since it is on par with the highest ^{60}Fe/^{56}Fe$_{CCAI}$ ratios estimated previously based on in situ measurements. Since IVB and IID irons isotopically belong to the carbonaceous meteorites, whereas all other samples measured as bulk, and almost all other samples measured in situ belong to the non-carbonaceous meteorites [14,15], IVB and IID irons may attest to ^{60}Fe heterogeneity in the early Solar System. Nevertheless, the magnitude of this heterogeneity is ill-constrained, because the ^{60}Ni-deficits calculated for the IVB and IID irons are model-dependent. Furthermore, despite the high ^{60}Fe/^{56}Fe$_{CCAI}$ ratios estimated for the IVB and IID precursors, the discrepancy between ^{60}Fe/^{56}Fe ratio estimates based on bulk and in situ isotope data remains, because the highest ^{60}Fe/^{56}Fe$_{CCAI}$ ratios estimated from in situ isotope measurements are based on chondrule and troilite data from unequilibrated ordinary chondrites (UOCs), which are isotopically non-carbonaceous, like angrites and basaltic eucrites for which bulk studies found low initial abundances of ^{60}Fe (see above).

The reasons behind the different ^{60}Fe/^{56}Fe ratios inferred from in situ and bulk data can be unrecognized isobaric interferences, the disturbance of the Fe-Ni system, as well as the inclusion of material in the analyses genetically unrelated to the target minerals [e.g., 16]. Some of these issues can be addressed by a better spatial control of in situ measurements, and the subsequent nanoscale investigation of the mineralogy and chemistry of the analyzed phases. To this end, and to better understand the ^{60}Fe-abundance systematics of the early Solar System in general, we have been carrying out in situ, high spatial resolution Fe-Ni isotope measurements on chondritic troilite and silicates with the NanoSIMS [e.g.,17], and studying electron-transparent slices of some of the minerals after isotope analysis, using transmission electron microscopy. In the past year we have expanded our dataset, which now indicates a resolvable, small ^{60}Fe/^{56}Fe ratio in the early Solar System, similar to the ^{60}Fe/^{56}Fe ratios inferred from the isotope data of bulk samples.

Samples and Analytical Methods: We studied 5 petrologic type 3.00–3.05 UOCs and CO carbonaceous chondrites, with minimal signs of aqueous alteration (Northwest Africa 8276, Queen Alexandra Range 97008, Meteorite Hills 00526, Allan Hills A77307, Dominion Range 08006), and the slightly more altered UOC Semarkona. We selected olivine, enstatite, and troilite for isotope analysis, with high Fe/Ni ratios (usually several thousand, or more), which we estimated from energy dispersive X-ray spectroscopy (LEO 1530 scanning electron microscope, Oxford X-Max 80 mm² detector; Max Planck Institute for Chemistry, Mainz, Germany) and electron probe microanalysis (JEOL JXA 8530F; University of Münster).

Isotope measurements were performed using the NanoSIMS 50 of the Max Planck Institute for Chemistry. We used a 75–500 pA O^- primary ion beam (Hyperion source) to scan 2×2 µm² to 6×6 µm² areas of the target minerals. The primary beam diameter was usually ~200 nm, but for a few measurements a ~1 µm diameter beam was used. We recorded positive secondary ions of ^{28}Si (troilite) or ^{29}Si (silicates), ^{46}Ti/^{46}Ca, ^{54}Fe, ^{60}Ni, and ^{62}Ni simultaneously, using electron multipliers. The mass resolution (M/ΔM) was tuned to 4,000–5,000 for masses 60 and 62, and we

measured ^{60}Ni and ^{62}Ni about −1.2 milli atomic mass units off their peak centers, which reduced the effects of isobaric interferences to negligible levels. We performed most of our analyses in imaging mode, which allowed the selection of vein- and inclusion-free, as well as Ti/Ca-poor regions of interest during data reduction.

Electron-transparent slices of selected troilites and silicates analysed by the NanoSIMS were investigated with the image-corrected FEI/ ThermoFisher Themis transmission electron microscope (University of Münster), operated at an acceleration voltage of 300 kV.

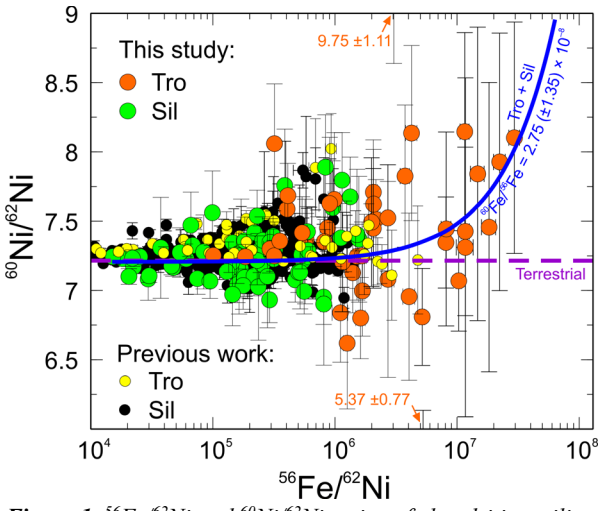

Figure 1. *^{56}Fe/^{62}Ni and ^{60}Ni/^{62}Ni ratios of chondritic troilites and silicates (data from in situ measurements), with 1σ uncertainties. Blue line was calculated from weighted linear regression of our combined troilite + silicate data, following [18]. Literature data are from [3,7–10,19,20].*

Results and Discussion: The Fe/Ni ratios of the analyzed troilites and silicates were between 4,000 and 1,170,000, and between 600 and 62,400, respectively. Neither individual troilite grains, nor chondrules showed resolvable signs of in situ ^{60}Fe decay, because of the often low number of analysis points that could be measured. However, pooled data show a resolvable (>2σ) slope in the ^{60}Ni/^{62}Ni vs. ^{56}Fe/^{62}Ni space (weighted linear regression followed [18]), 2.75 (±1.35) × 10^{-8} (Figure 1), which can be interpreted as the average initial ^{60}Fe/^{56}Fe ratio of the analyzed minerals. This result is more consistent with the low initial ^{60}Fe/^{56}Fe ratios inferred for angrites, eucrites and bulk chondrules, than the high initial ^{60}Fe/^{56}Fe ratios inferred for certain chondrules and troilites from previous in situ measurements (see above). The average initial ^{60}Fe/^{56}Fe ratios inferred for our carbonaceous and non-carbonaceous samples (2.49 (±1.37) × 10^{-8} and 1.47 (±0.93) × 10^{-7}, respectively) cannot be distinguished from each other at the 95 % confidence level, and UOC silicates and troilites seem to have had a higher initial ^{60}Fe/^{56}Fe ratio on average, than their counterparts in our carbonaceous meteorites. Based on literature data on bulk meteorites (^{60}Fe/^{56}Fe$_{CCAI}$ of carbonaceous reservoir > ^{60}Fe/^{56}Fe$_{CCAI}$ of non-carbonaceous reservoir, see above), and assuming that the average age of the analyzed carbonaceous and non-carbonaceous meteorite components is similar, this is unexpected.

Transmission electron microscopy could confirm that the high Fe/Ni phases have not lost substantial amounts of Ni, or gained Fe after crystallization. We occasionally observed Ni-rich veins that crosscut some of the analyzed minerals (cf. [16]), but we have not seen evidence for element transport between the veins and their hosts, such as zoning, or Ni-poor or Ni-rich patches within the hosts along the veins. Using the imaging mode of the NanoSIMS, the Ni-rich veins can usually be avoided during data reduction, and even if included in the analyzed volume, they should not change the inferred ^{60}Fe/^{56}Fe ratios. The high Fe/Ni ratios of the analyzed troilites and silicates are thus unlikely to be related to grain boundary diffusion or fluid transport, as suggested by [16]. We are therefore confident that the low inferred initial ^{60}Fe/^{56}Fe ratios of our troilites + silicates by and large are not the result of sub-solidus re-equilibration.

Acknowledgements: Our project was financially supported by the German Research Foundation (DFG) Special Priority Programme 1833 (grants no.: HO2163/3-1, VO1816/4-1). Thin sections of QUE 97008, MET 00526, ALHA77307, and DOM 08006 were provided by the Antarctic Search for Meteorites (ANSMET) program (NSF, NASA).

References: [1] Rugel G. et al. (2009) *PRL, 103*, 072502. [2] Neumann W. et al. (2018) *JGR:P, 123*, 421–444. [3] Mostefaoui S. et al. (2005) *ApJ, 625*, 271–277. [4] Quitté G. et al. (2010) ApJ, 720, 1215–1224. [5] Tang H. and Dauphas N. (2012) *EPSL, 359–360,* 248–263. [6] Tang H. and Dauphas N. (2015) *ApJ, 802*, 22. [7] Mishra R. K. and Chaussidon M. (2014) *EPSL, 398*, 90–100. [8] Mishra R. K. and Goswami J. N. (2014) *GCA, 132*, 440–457. [9] Mishra R. K. et al. (2016) *EPSL, 436*, 71–81. [10] Telus M. et al. (2018) *GCA, 221*, 342–357. [11] Trappitsch R. et al. (2018) *ApJL, 857*, L15. [12] Steele R. C. J. et al. (2012) *ApJ, 758*, 59. [13] Cook D. L. (2021) *ApJ, 917*, 59. [14] Warren P. H. (2011) *EPSL, 311*, 93–100. [15] Nanne J. A. M. et al. (2019) *EPSL, 511*, 44–54. [16] Telus M. et al. (2016) *GCA, 178*, 87–105. [17] Kodolányi J. et al. (2021) *52nd Lunar and Planetary Science Conference*, Abstract #1291. [18] Mahon K. I. (1996) *Intl. Geol. Rev., 38*, 293–303. [19] Tachibana S. and Huss G. R. (2003) *ApJ, 588*, L41–L44. [20] Telus M. et al. (2012) *MAPS, 47*, 2013–2030.